

*The Deuteron: Structure and Dynamics from Data on  
Fragmentation with Large Proton Transverse Momenta*

L.S. Azhgirey

JINR, Dubna, Russia

## Introduction

---

The deuteron occupies a particular place among nuclei because it is the simplest loosely bound system of two nucleons in  ${}^3S_1$  and  ${}^3D_1$  states. Deuteron static properties (binding energy, electric quadrupole moment, magnetic dipole moment, and so on) are known with high accuracy, and they are well reproduced in the framework of non-relativistic calculations on the basis of  $NN$  potentials of the one-boson exchange. The nonrelativistic DWF obtained from the solution of the Schrödinger equation depends only on the relative momentum of nucleons  $\mathbf{q}$ :  $\Psi = \Psi(\mathbf{q})$ . Two components of the non-relativistic DWF presenting the  $S$  and  $D$  states are dominant at large and small distances between nucleons, respectively.

## Infinite Momentum Frame

---

- As energies of a deuteron and their nucleons increase, **relativistic effects** come into play. In view of the fact that a relativistic boost depends on an interaction (in the familiar instant form dynamics), at relativistic energies there is a problem that it is impossible to separate the motion of the system as a whole from the relative motion of constituents. A relativistic WF turns out to be dependent not only on the relative momentum of nucleons  $\mathbf{q}$ , but on the total momentum  $\mathbf{p}$  of the center inertia movement of the system as well:  $\Psi = \Psi(\mathbf{p}, \mathbf{q})$ . So, the relativistic WF is the function of  $\mathbf{q}$  for each new reference system.
- On the other hand, it is sufficient to know the WF in the limit of the infinite momentum  $\mathbf{p} \rightarrow \infty$  [**Weinberg**]

## Relativistic Wave Function

---

- The structure of WF is simplified in the IMF: the dependence on  $|\mathbf{p}|$  disappears, only the dependence on the direction  $\mathbf{n} = \mathbf{p}/|\mathbf{p}|$  remains.
- So, relativistic WF is the function of two variables:  $\Psi = \Psi(\mathbf{q}, \mathbf{n})$ . The same results when employing the light-front dynamics [**Dirac**].
- Additional advantage of this approach is the disappearance of the so-called **z-diagrams**, in consequence the concept of wave function having a probabilistic meaning may be used. An appropriate formalism to describe relativistic properties of the deuteron was developed by Karmanov et al. [**Karmanov**].

# Relativistic Quantum Theory

---

- Another approach to treat relativistic composite systems is based on special insertion of the interaction into the Hamiltonian theory of two- and three-particle systems, so that the relevant Schrödinger equation turns out to be relativistic invariant ( **the relativistic quantum theory**) [**Coester,Keister,Yu.Uzikov**]. Here the wave function also does not depend on the total momentum of the deuteron and therefore the internal motion may be separated from the external one.
- However, nowadays the employment of this approach to describe the microworld physics is restricted, because there are no necessary number of parameters, functions etc. to judge correctness and usefulness of the results.

# Bethe-Salpeter Equation

---

- One further approach realizes at the modern level ideas similar to the underlying ideas of the Bethe-Salpeter and Dyson equations [**Tijon, Burov, Kaptari et al.**].
- Despite the undoubted significance of this approach, it is likely seriously restricted by the inevitable necessity of a certain specification of irreducible diagram blocks.
- Thus, at the moment there are different approaches to treating the relativistic properties of composite systems.

## Concept of Dynamics

---

- For understanding the physics of relativity, it was very important to realize the significance of the concept of dynamics introduced by P.A.M.Dirac [**Dirac**].
- The relativistic quantum theory and field theory can be formulated in any one of these forms of dynamics, and the final physical results of analysis of phenomena within each dynamics should be identical. However, it is quite possible that the description of the physics of phenomena in different dynamics may be different; in particular, it may appear simpler in one of them.
- Generally speaking, at least three of ten generators of Poincaré group are dynamical resulting in a violation of invariance about one or other transformations, and one is forced to restore this invariance by one or other means.

## Forms of Dynamics

---

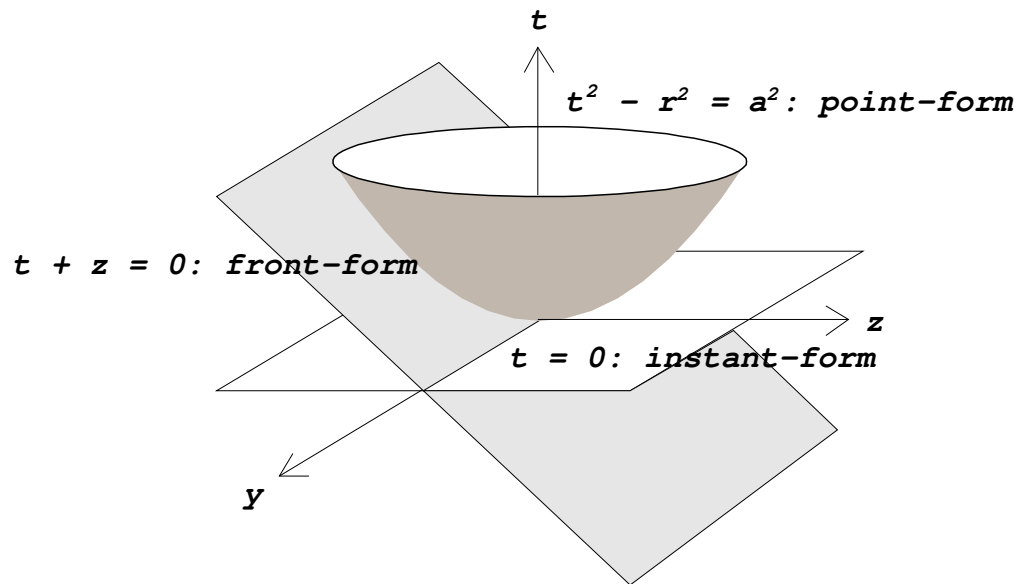
- Each form of dynamics is associated with **a hypersurface** on which the commutation relations for the generators of Poincaré group are defined, or the way the 10 generators are split into **kinematical** and **dynamical** ones.

## Forms of Dynamics

- Each form of dynamics is associated with a **hypersurface** on which the commutation relations for the generators of Poincaré group are defined, or the way the 10 generators are split into **kinematical** and **dynamical** ones.

forms of dynamics	kinematical generators	dynamical generators
<b>time instant</b>	$p_1, p_2, p_3$ $J_1, J_2, J_3$	$p_0$ $K_1, K_2, K_3$
<b>light front</b>	$p^+ = p_0 + p_3, p_1, p_2$ $E_1 = \frac{1}{2}(K_1 + J_2)$ $E_2 = \frac{1}{2}(K_2 - J_1)$ $K_3, J_3$	$p^- = p_0 - p_3$ $F_1 = K_1 - J_2$ $F_2 = K_2 + J_1$

# Hypersurfaces of Different Forms of Dynamics



In place of the usual spatial coordinate system  $(t, x, y, z)$ , light-front dynamics makes use of the light-front coordinate system  $(x^+, x^-, x, y)$ , with  $x^\pm = t \pm z$ . A four-vector is expressed as  $(p^+, p^-, p_1, p_2)$ , where  $p^\pm = p_0 \pm p_3$ .

## Karmanov's Model in the LF Dynamics

---

- In Karmanov's approach the problem of rotational invariance is solved by including the orientation of the light-front hyperplane in the number of additional dynamic variables.
- Because of this the simultaneous rotation of the dynamic variables of the system and the light-hyperplane orientation should not lead to a change in the physical content of the theory. This means that the state vectors of the system in such an operation are transformed with the help of an interaction-independent rotation operator.
- Consequently, it turns out that a certain relation is established between the rotation operators for dynamic variables of the system and quantization plane.

## Karmanov's Relativistic DWF

---

- The rotation operator for the quantization plane is only geometrical, i.e., independent of the interaction. As a result, the problem of the total angular momentum becomes only geometrical, and it is possible to construct beforehand the states with a certain angular momentum.
- Thus, Karmanov's observation consists in the fact that the interaction-dependent part of the operators  $J_x$  and  $J_y$  is simply equal to the rotation operator of the quantization plane
- In the framework of this approach, an explicitly covariant relativistic DWF was constructed [**Carbonell, Karmanov**]. It is defined by the six invariant functions, each being dependent on two variables.

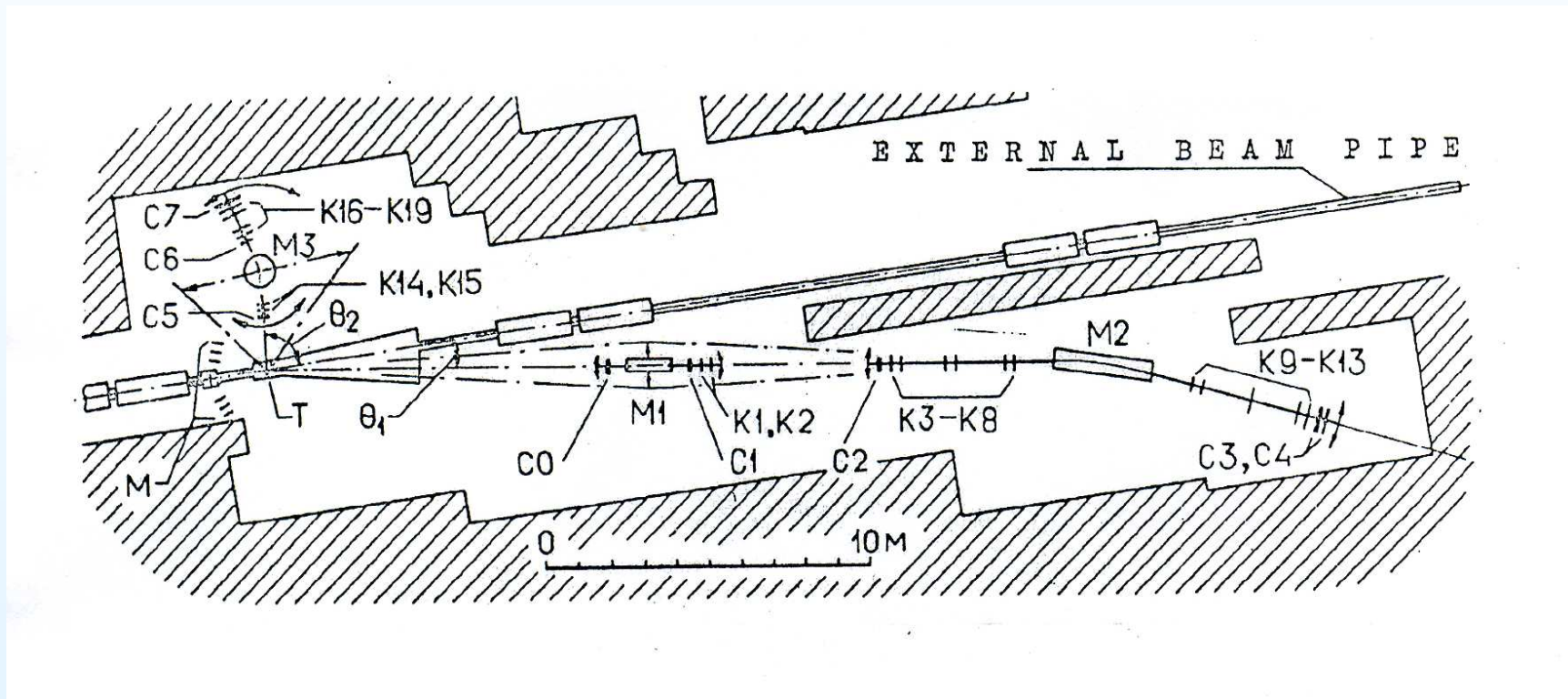
# Hadronic Deuteron Break-up at High Energy

---

- Measurements of the inclusive reaction  $A(d, p)X$  with high-energy deuterons provide a handy way to study the deuteron short-range structure. A qualitative picture of this process at relativistic energies is described by the hard scattering model [**Blankenbecler et al.**]. The stripping predominates at very small angles of detection of protons, while the hard scattering (**elastic  $pp$  and exchange  $np$  scatterings**) manifest itself as these angles increase.
- Measurements of the momentum spectra of protons emitted with large transversal momenta in the interactions of 9-GeV $_c$  **deuterons** with **H, D and C** nuclei [**Azhgirey et al.**] have strengthened of this picture.

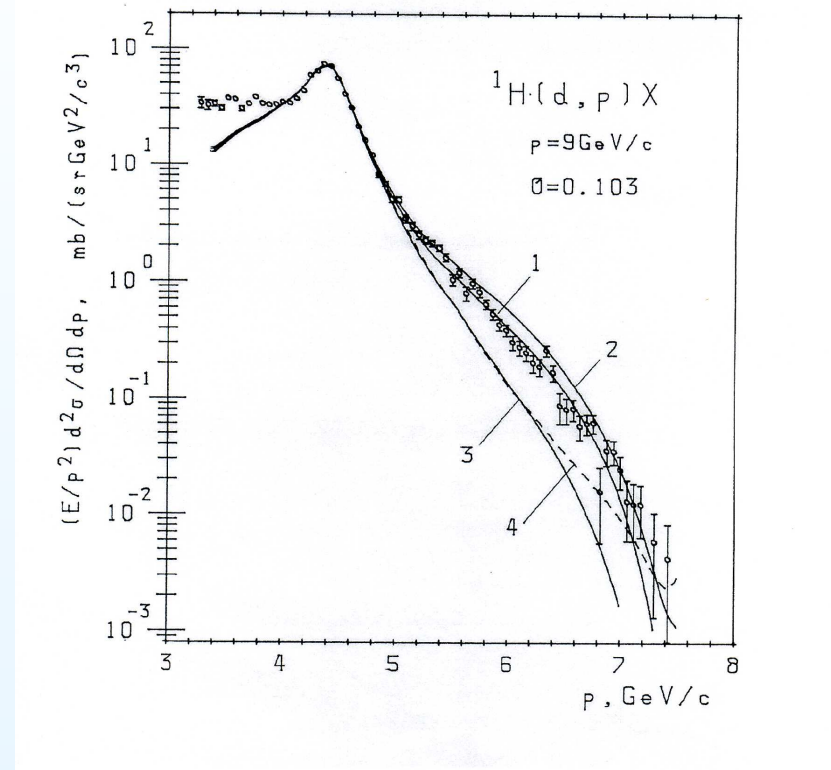
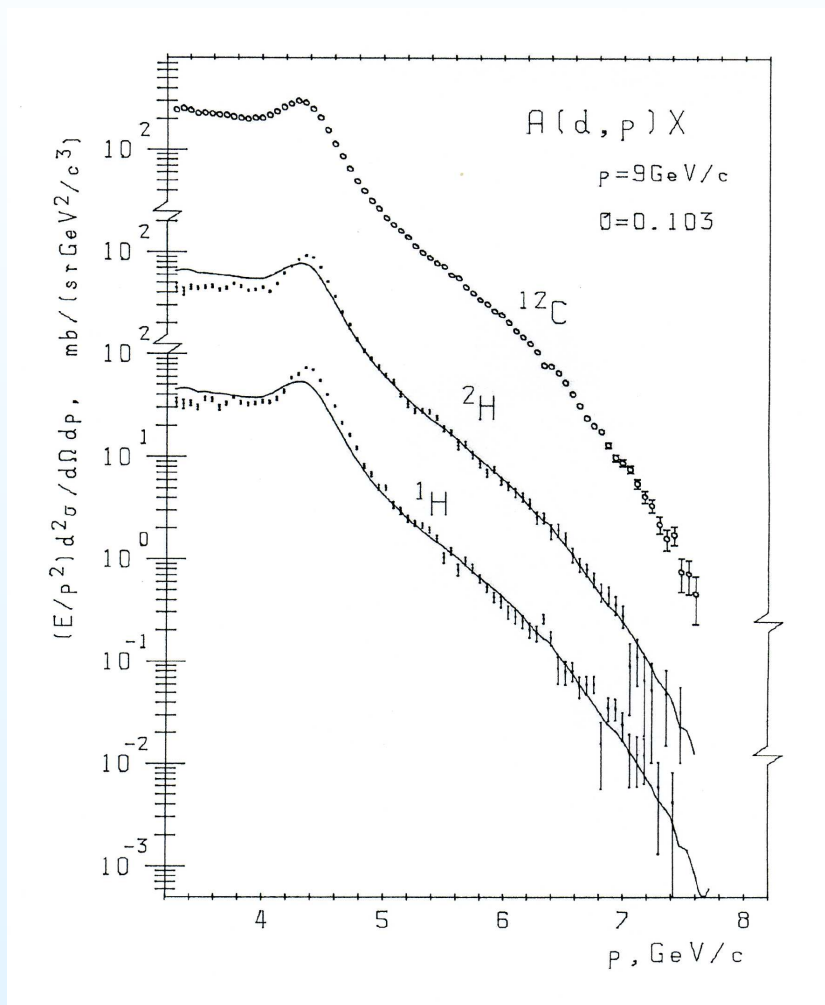
## Layout of the MASPIK Setup

Measurements of the momentum spectra of the deuteron breakup with the proton emission at nonzero angles were performed at the Dubna Synchrophasotron and the MASPIK setup [**L.S.Azhgirey et al., NP A528(1991)621**].





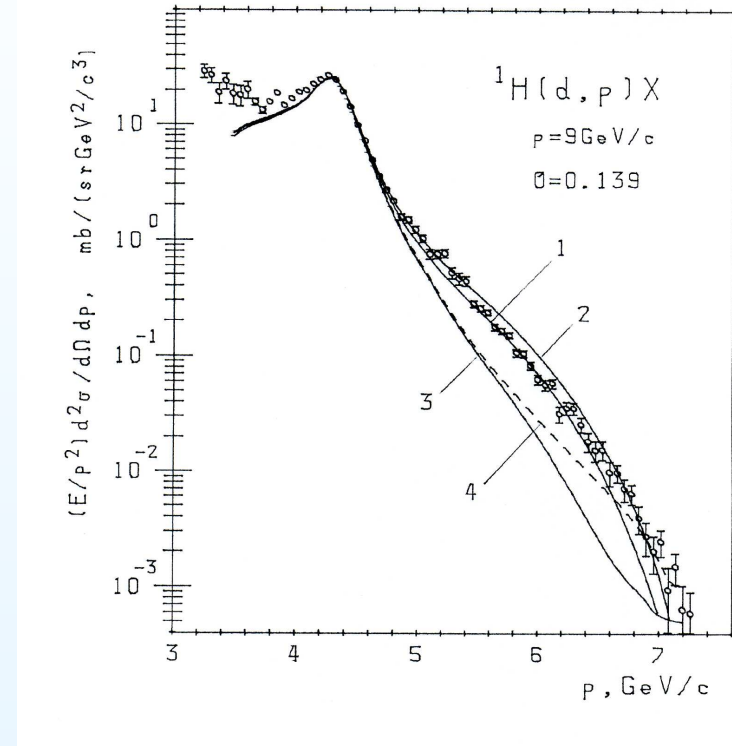
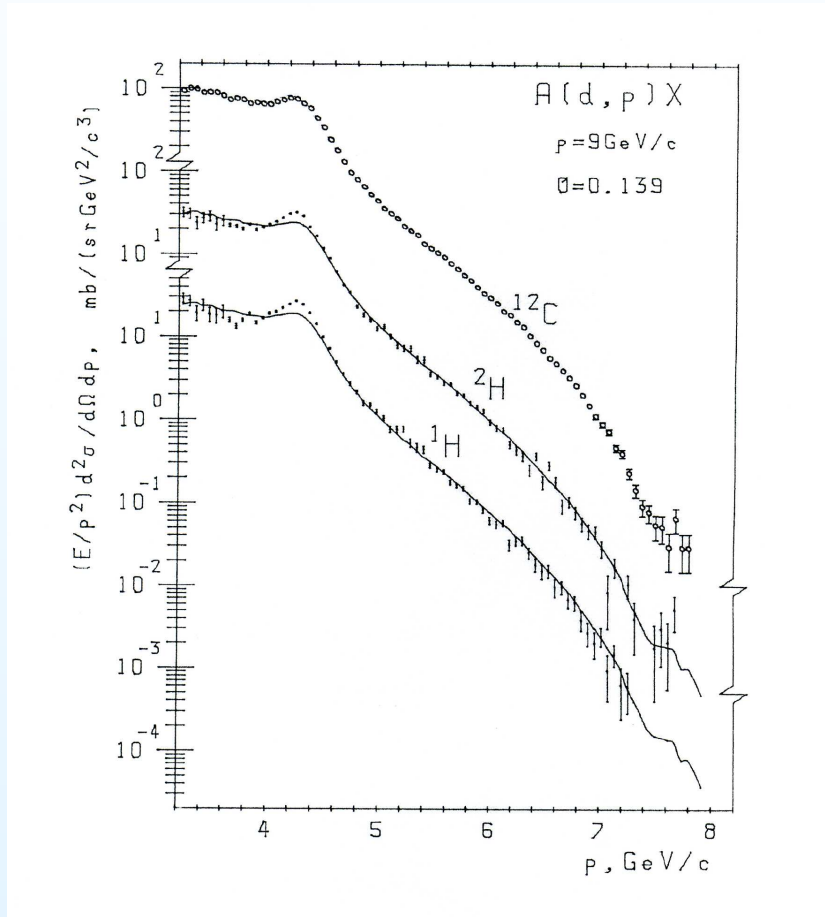
# Momentum Spectra of Protons at 103 mr



Deuteron wave functions:

1 - for Paris potential; 2 - for Reid SC potential; 3 - for Bonn A potential; 4 - for Bonn B potential.

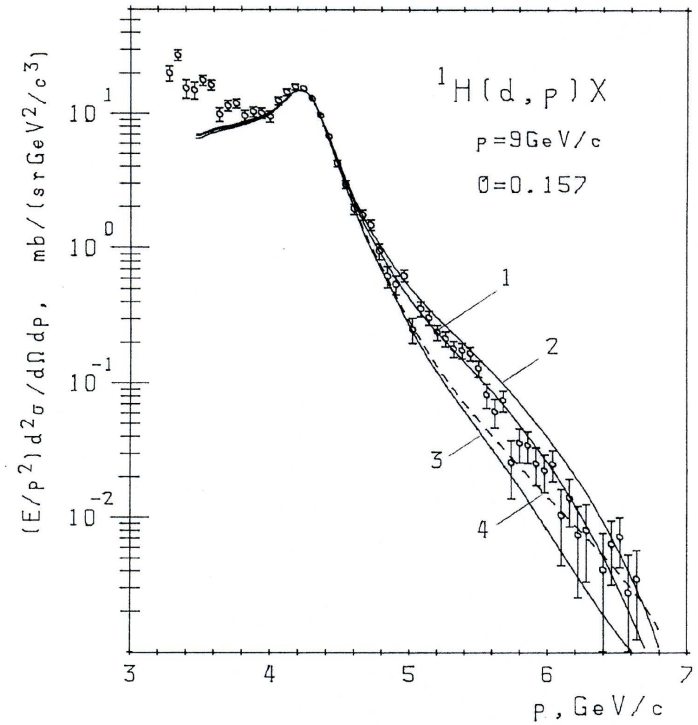
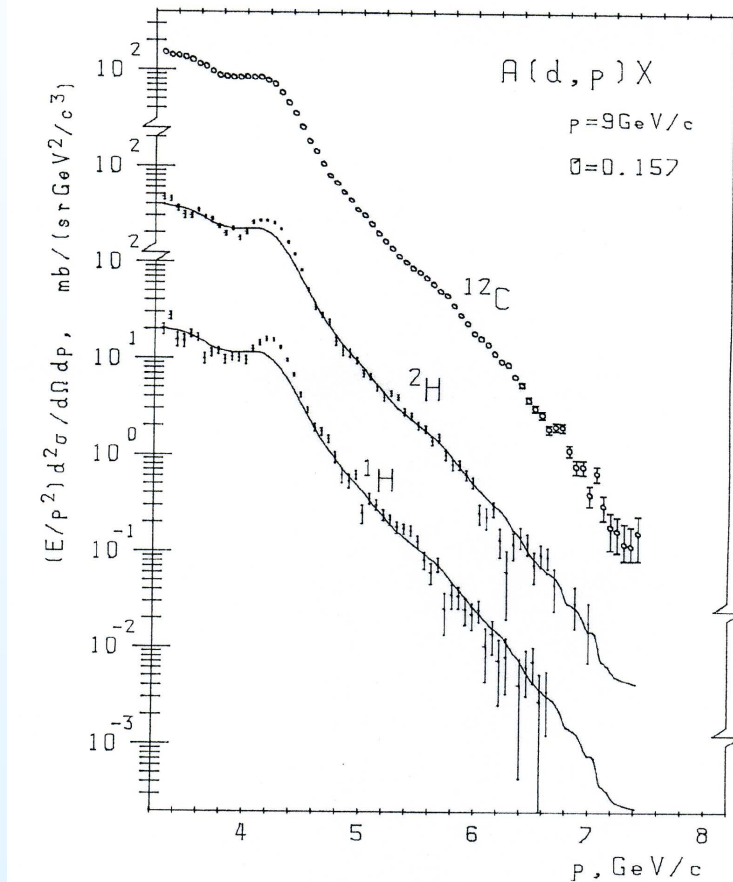
# Momentum Spectra of Protons at 139 mr



Deuteron wave functions:

1 - for Paris potential; 2 - for Reid SC potential; 3 - for Bonn A potential; 4 - for Bonn B potential.

# Momentum Spectra of Protons at 157 mr



Deuterin wave functions:

- 1 - for Paris potential;
- 2 - for Reid SC potential;
- 3 - for Bonn A potential;
- 4 - for Bonn B potential.

## From Cross-sections to Polarization Measurements

---

- The construction of the polarized-deuteron source **POLARIS**] and the realization of acceleration of the polarized-deuteron beam at the JINR synchrophasotron made it possible to perform a series of experiments on measuring the polarization properties of the process of nuclear interactions with relativistic deuterons.
- Investigation of polarization observables in the reactions with the participation of high-energy deuterons is especially suitable for clarifying the deuteron structure at the relativistic momenta of its components because these observables are more sensitive to deuteron properties than the momentum distributions.

## Failure of Non-relativistic Description

---

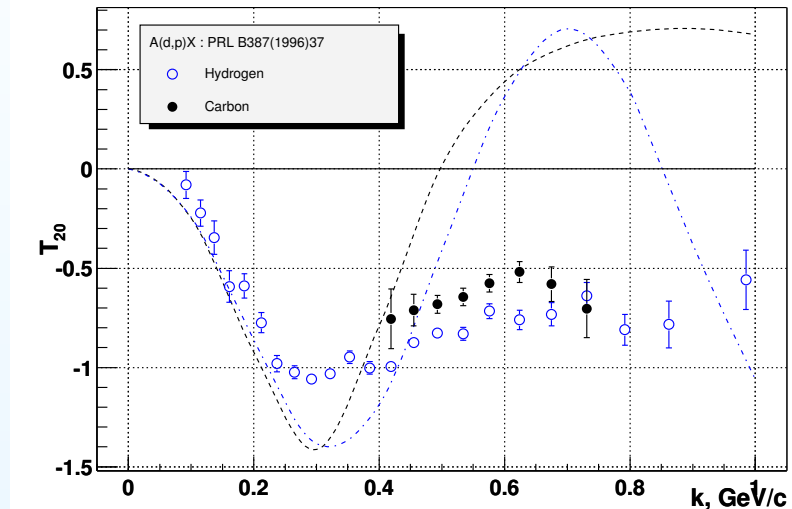
Investigations of polarization properties of the deuteron fragmentation reaction  $(d, p)$  [Saclay; Dubna] have amassed a convincing body of evidence that the description of the deuteron structure by means of wave functions derived from non-relativistic functions through **the kinematical transformation of variables** is liable to break down at short distances between nucleons. The main discrepancies between the expected and observed behaviour of data manifest themselves in the following facts.

## $T_{20}$ of Deuteron Breakup vs $k$

The expression for the tensor analyzing power  $T_{20}$  of deuteron breakup in the impulse approximation has the form

$$T_{20} \sim w(k)[\sqrt{8}u(k) - w(k)],$$

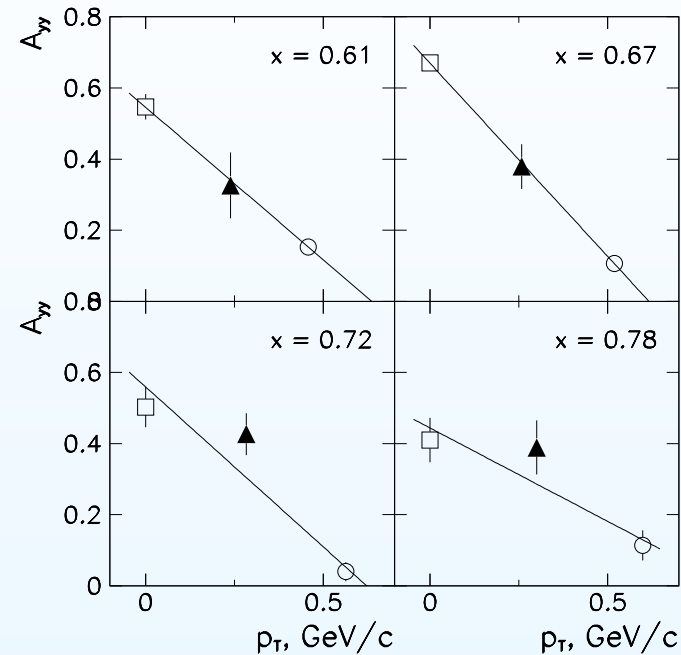
where  $u(k)$  and  $w(k)$  are the deuteron momentum space wave functions for  $S$  and  $D$  states, respectively, and  $k$  is the internal momentum of the nucleons in the deuteron. With standard deuteron wave functions, the  $T_{20}$  dependence on  $k$  can be expected to change the sign at  $k \sim 0.5$  GeV/c, but this expectation lacks support from experiment.



The  $T_{20}$  dependence on  $k$  in inclusive deuteron breakup at 9 GeV/c and  $0^\circ$  on hydrogen and carbon [**L.S.Azhgirey et al., PLB 387(1996)37**].

## $A_{yy}$ of Deuteron Break-up vs $p_T$

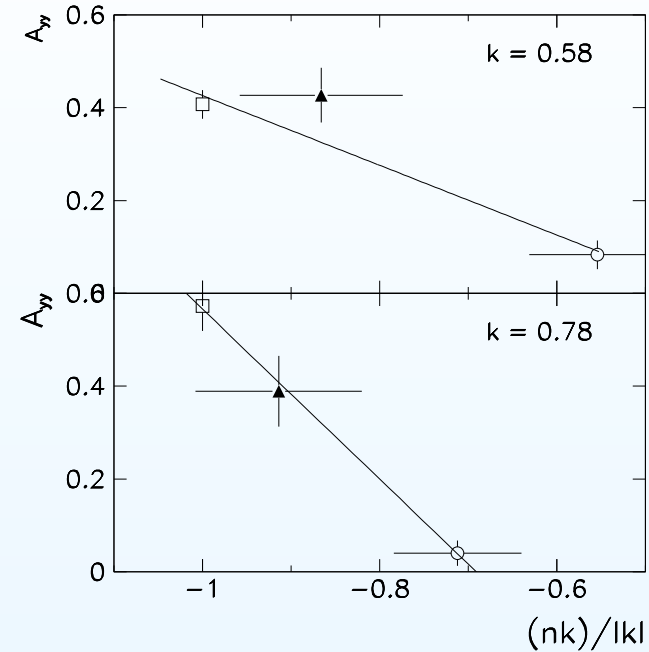
The recent measurements of the tensor analyzing power  $A_{yy}$  of the breakup of relativistic deuterons on nuclei at non-zero angles of emitted protons [L.S.Azhgirey et al., *YaF* 66(2003)719] show that the measured  $A_{yy}$ -values at fixed value of the longitudinal proton momentum have the dependence on the transverse proton momentum  $p_T$  that differs from that calculated with standard deuteron wave functions.



$A_{yy}$  data vs  $p_T$  at fixed  $x = 0.61, 0.66, 0.72,$  and  $0.78$ . The open circles, solid triangles, and open squares represent the data at  $9 \text{ GeV}/c$  and  $0^\circ$ ,  $4.5 \text{ GeV}/c$  and  $80 \text{ mr}$ , and  $9 \text{ GeV}/c$  and  $85 \text{ mr}$ , respectively.

## $A_{yy}$ of deuteron breakup vs $(\mathbf{n} \cdot \mathbf{k})$

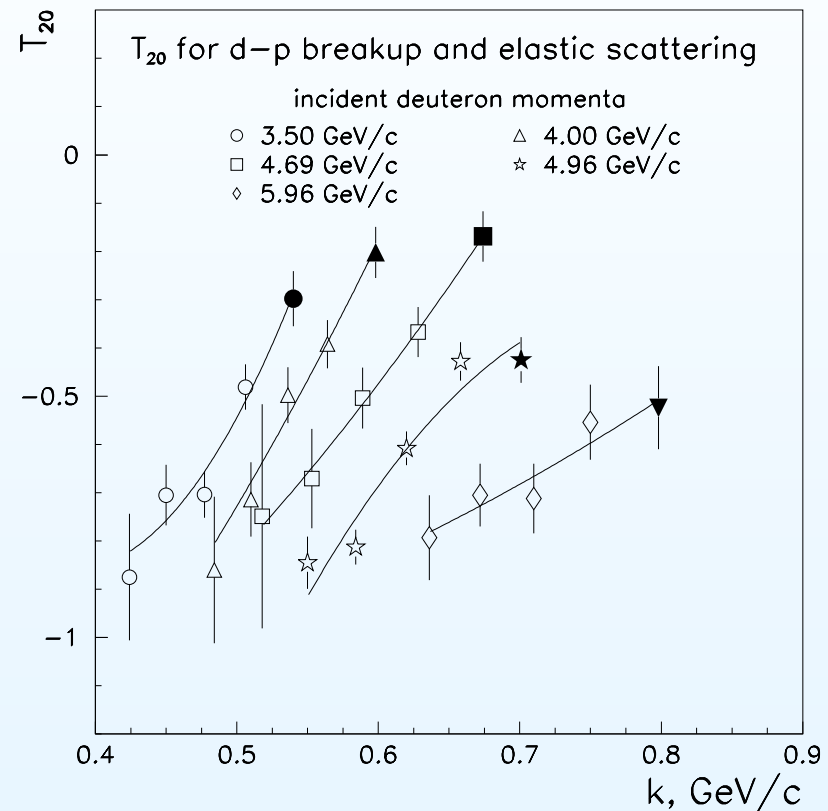
The above-mentioned data show that the values of  $A_{yy}$  being plotted at fixed values of  $k$  tend to decrease as the variable  $(\mathbf{n} \cdot \mathbf{k})$  grows (vector  $\mathbf{n}$  is the unit normal to the surface of the light front).



$A_{yy}$  data vs the  $(\mathbf{n} \cdot \mathbf{k})$  variable at fixed  $k$  of  $\sim 560$  and  $\sim 740$  MeV/ $c$ . The open circles, solid triangles, and open squares represent the data obtained at 9 GeV/ $c$  and  $0^\circ$ , 4.5 GeV/ $c$  and 80 mr, and 9 GeV/ $c$  and 85 mr, respectively.

# Pion-free Deuteron Breakup Process

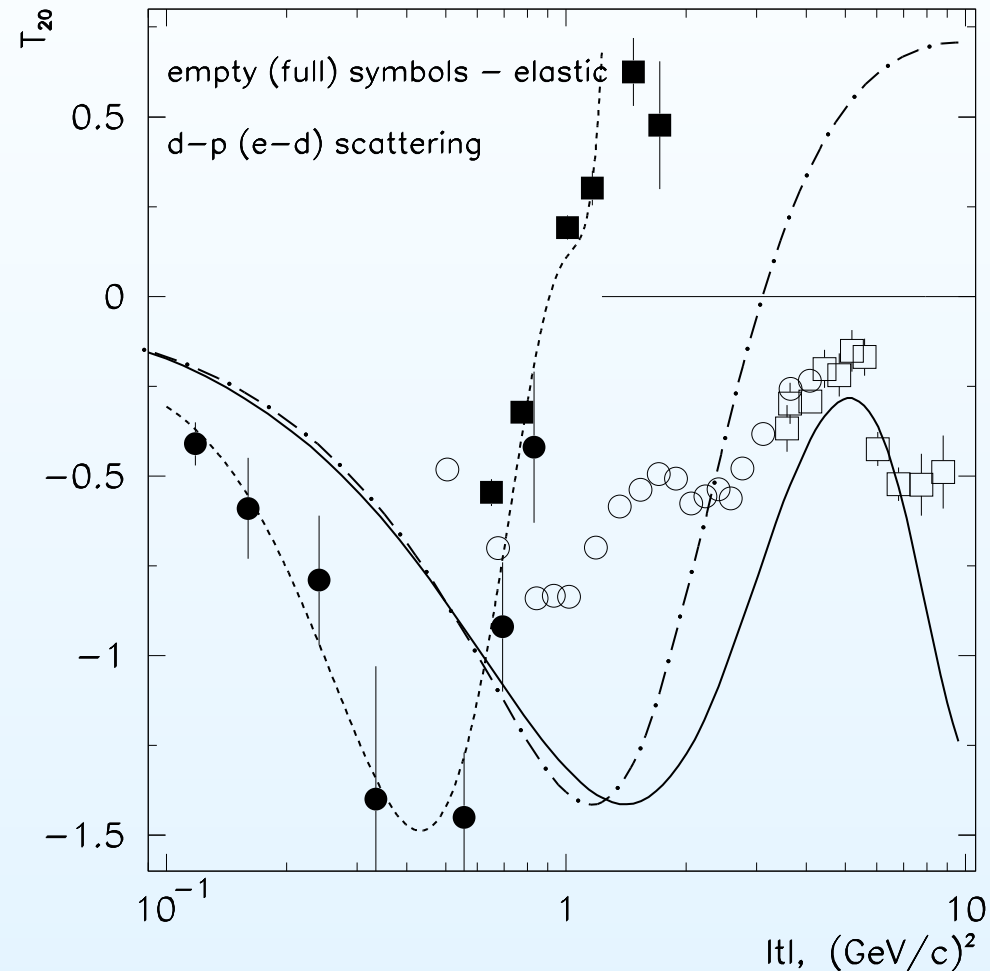
The pion-free deuteron breakup process  $dp \rightarrow ppn$  in the kinematical region close to that of backward elastic  $dp$  scattering at a given value of  $k$  depends on the incident momentum of deuteron [**L.S.Azhgitey et al. PLB 44(1997)444**]



The  $T_{20}$  dependence of deuteron breakup on  $k$  at different initial deuteron momenta.

# Investigations with EM Probes

It should be noted that different aspects of deuteron structure are explored by means of electromagnetic and hadron probes. To realize this, it is instructive to compare  $t$ -dependencies of the tensor analyzing power  $T_{20}$  for elastic  $ed$  [M.Garcon et al.; D.Abbott et al.] and backward  $dp$  [V.Punjabi et al.; L.Azhgirey et al.] scatterings.



## Data on the Deuteron Breakup

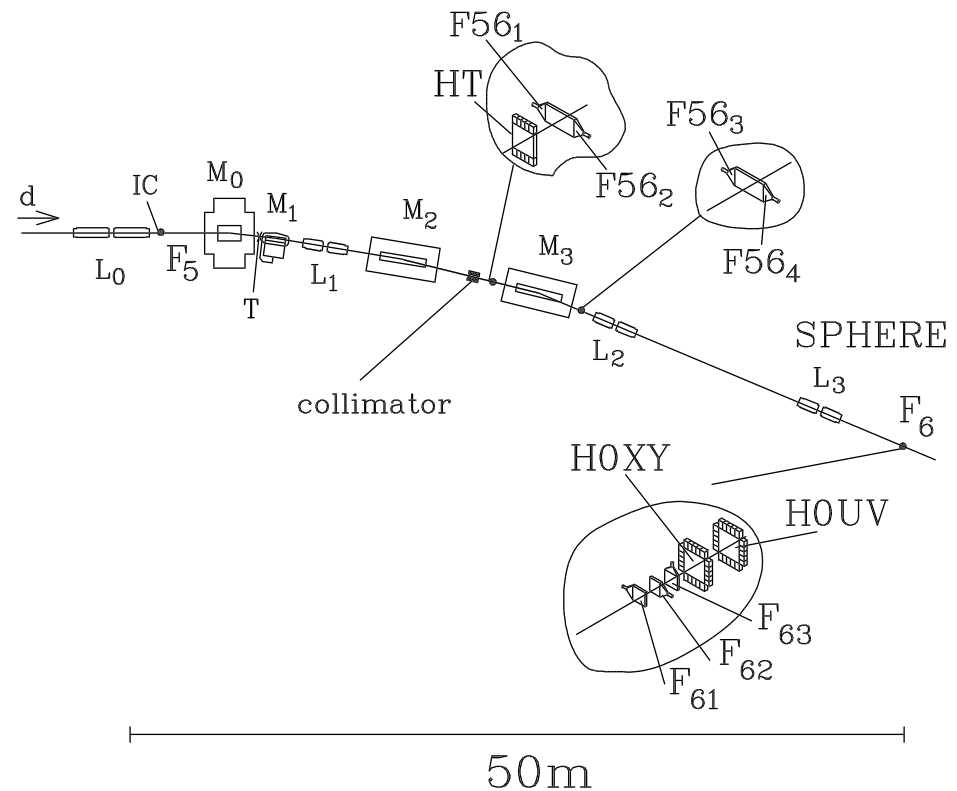
Let us compare the data on the tensor analyzing power  $A_{yy}$  of  $(d, p)$  reaction with predictions of a relativistic description based on the light-front dynamics.

In the region of large transverse momenta, parameter  $A_{yy}$  of the deuteron breakup on nuclei was measured at the following conditions.

deuteron momentum, GeV/c	proton emission angle, mrad	target	reference
9	85	$^{12}\text{C}$	Afanasiev et al., PL B434(1998)21 Azhgirey et al., YF 62(1999)1796
4.5	80	$^9\text{Be}$	Ladygin et al. F-B Syst. 32(2002)127 Azhgirey et al., YF 66(2003)719
5	180	$^9\text{Be}$	Azhgirey et al., PL B595(2004)151
9	85, 130, 160	$^1\text{H}, ^{12}\text{C}$	Ladygin et al. PL B629(2005)60

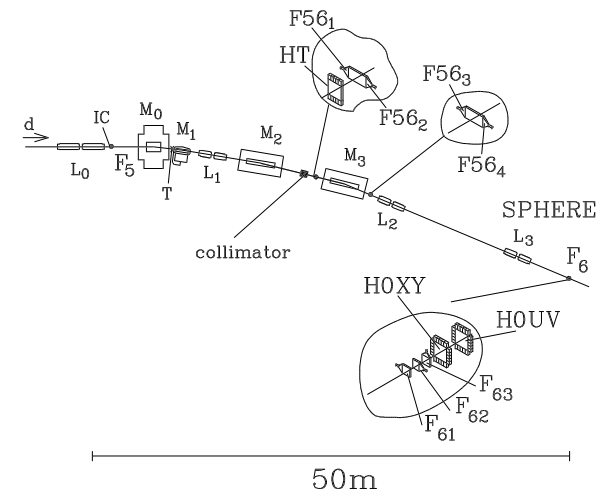
# Layout of Experiments

Experiments on the measurements of the tensor analysing power  $A_{yy}$  of the deuteron breakup with the proton emission at nonzero angles were performed with a polarized deuteron beam from the Dubna Synchrophasotron and the SPHERE setup described elsewhere [S.V.Afanasiev et al., PL B434(1998)21].

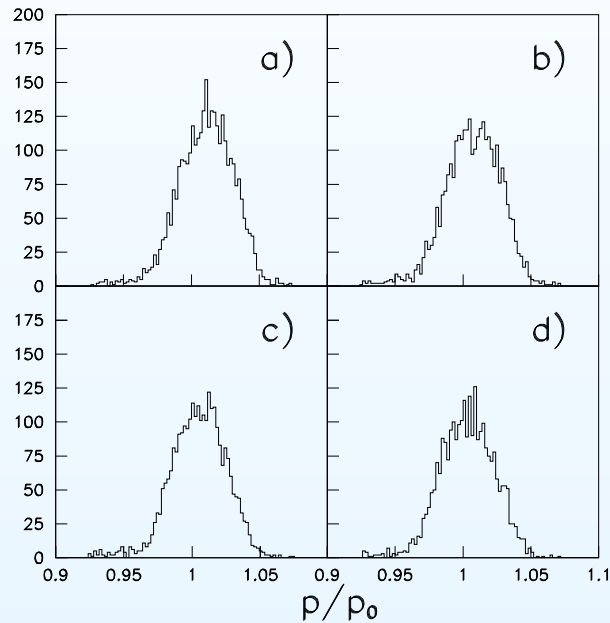


# Setup Characteristics in 5 GeV/c-Deuteron Run

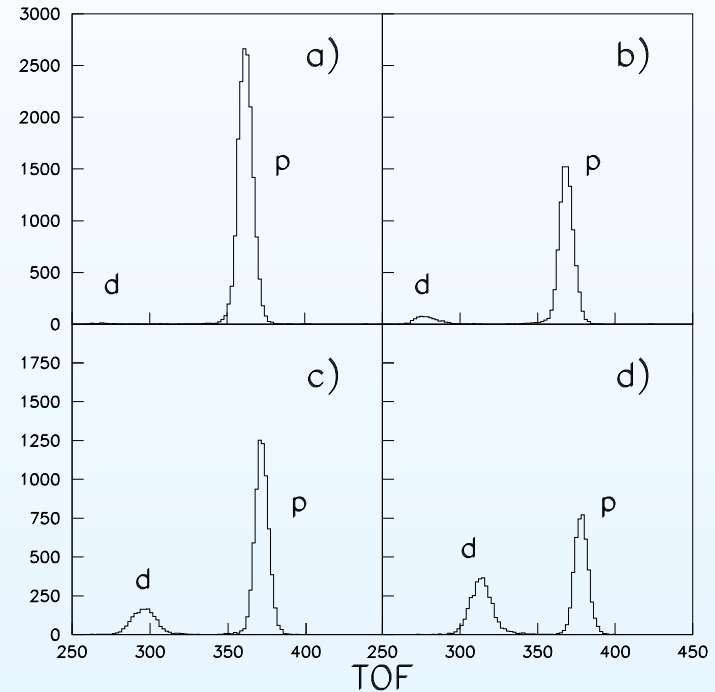
beam momentum	5 GeV/c
beam intensity	$5 \cdot 10^8$ d/spill
tensor polarization	$p_{zz}^+ = 0.716 \pm 0.043$ $p_{zz}^- = -0.756 \pm 0.027$
vector polarization	$p_z^+ = 0.173 \pm 0.008$ $p_z^- = 0.177 \pm 0.008$
beam sizes	$\sigma_x \sim 4mm, \sigma_y \sim 9mm$
target	Be, 16 cm thick
angle of detection	178 mr
momenta of secondaries	2.7, 3.0, 3.3, 3.6 GeV/c
momentum acceptance	$\Delta p/p \sim \pm 2\%$
polar angle acceptance	$\pm 18$ mr
TOF base line	28 m
TOF resolution	0.2 ns



# Acceptances, TOF

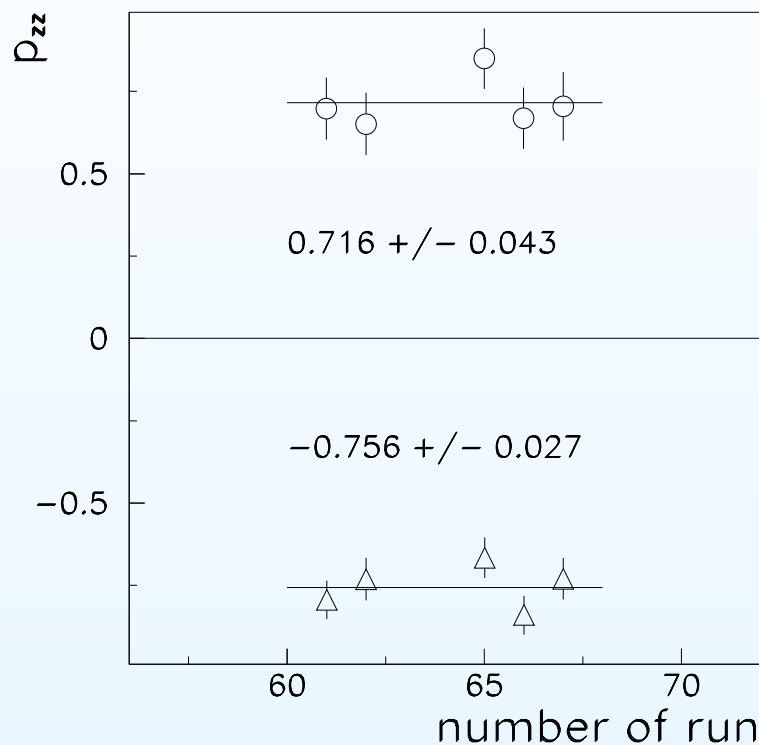


The momentum acceptances of the setup for protons at secondary proton momenta of 2.7, 3.0, 3.3, and 3.6 GeV/c.

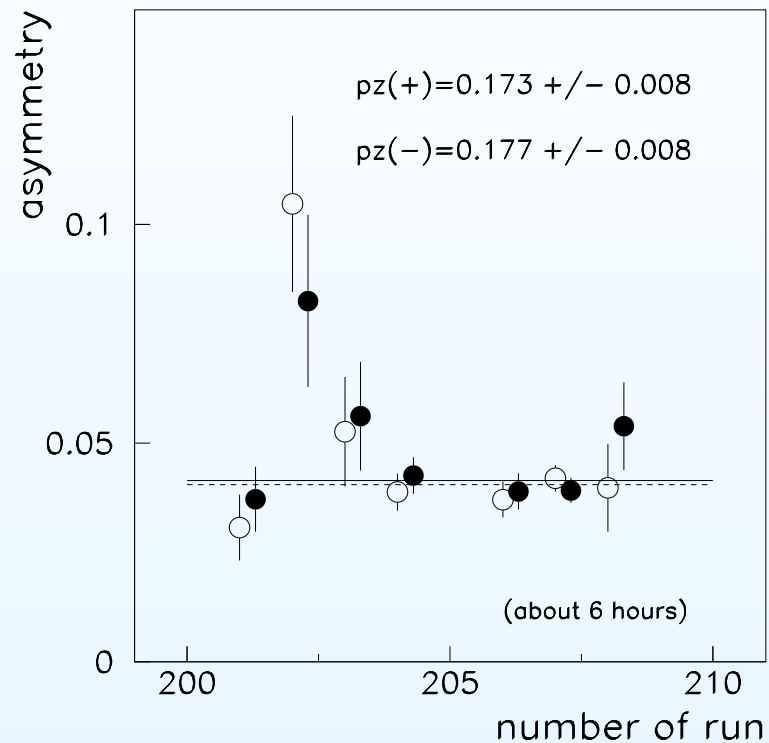


The TOF spectra for different magnetic elements tuning.

# Beam Polarizations



Tensor polarization of the deuteron beam in the experiment.



Asymmetry during monitoring vector component of the deuteron beam polarization.

## Necessity of an Additional Variable for Relativistic DWF

---

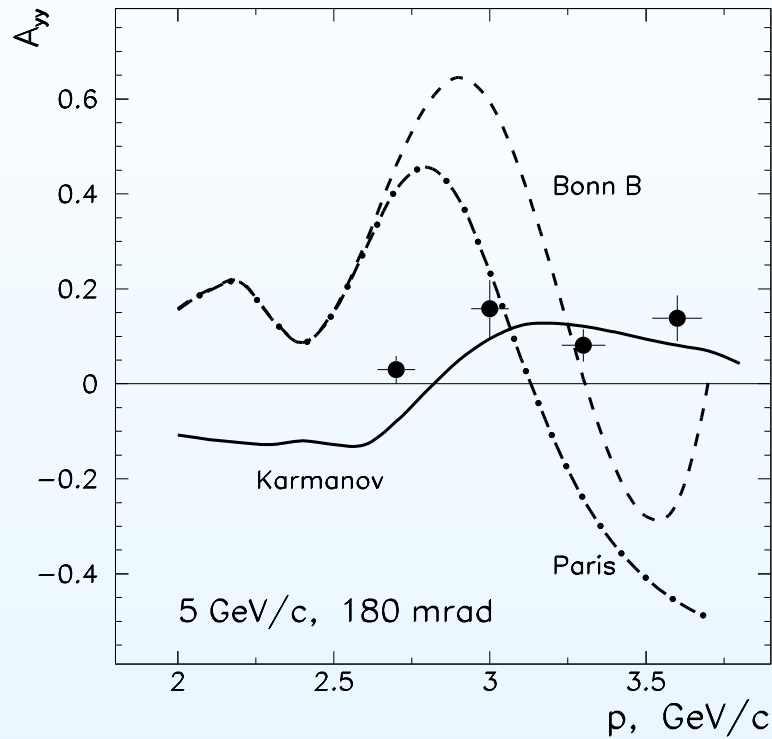
- From the comparison of the data obtained at 4.5 GeV/c [L.S.Azhgirey et al., YF 66(2003)719] with those at 9 GeV/c for the zero proton emission angle [L.S.Azhgirey et al., PL B387(1996)37] and a proton emission angle of 85 mrad [S.V.Afanasiev et al., PL B434(1998)21] it was concluded that the relativistic deuteron structure function needs to be described with two **independent** variables — longitudinal and transverse components of the internal motion momentum.

## Necessity of an Additional Variable for Relativistic DWF

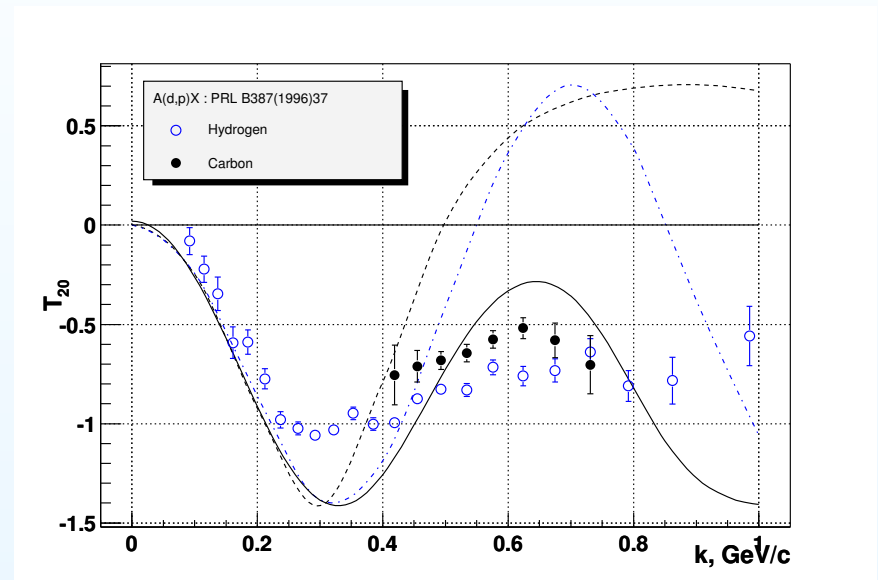
---

- From the comparison of the data obtained at 4.5 GeV/c [L.S.Azhgirey et al., YF 66(2003)719] with those at 9 GeV/c for the zero proton emission angle [L.S.Azhgirey et al., PL B387(1996)37] and a proton emission angle of 85 mrad [S.V.Afanasiev et al., PL B434(1998)21] it was concluded that the relativistic deuteron structure function needs to be described with two **independent** variables — longitudinal and transverse components of the internal motion momentum.
- On the other hand, the behaviour of the  $A_{yy}$  data at 5 GeV/c [L.S.Azhgirey et al., PL B595(2004)151] has been explained within the framework of the **LF dynamics** using Karmanov's relativistic deuteron wave function without invoking non-nucleonic degrees of freedom.

# Description with Karmanov's Relativistic DWF



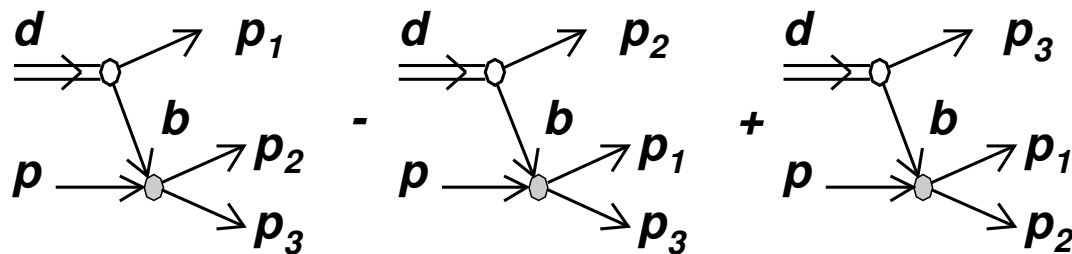
$A_{yy}$  of the reaction  ${}^9\text{Be}(d,p)X$  at  $5 \text{ GeV}/c$  and  $178 \text{ mr}$  vs detected proton momentum  $p$ .



$T_{20}$  of the  $(d,p)$  reaction on hydrogen and carbon at  $9 \text{ GeV}/c$  with the emission of protons at  $0^\circ$  vs internal momentum  $k$ .

# Mechanism of the Deuteron Breakup

The mechanism of the deuteron breakup on protons  ${}^1H(d,p)X$  can be in the simplest case represented by the Feynman diagrams:



Here  $d$  is the incoming deuteron,  $p$  is the target proton,  $b$  is the virtual off-shell nucleon,  $p_1$  is the detected proton, and  $p_2, p_3$  are nucleons. Diagram (a) corresponds to the case where the detected proton results from deuteron stripping, and at the low vertex elastic  $np$  scattering takes place. In diagrams (b) and (c) the low vertices correspond to the charge exchange  $np$  and elastic  $pp$  scatterings, respectively.

# Tensor Analyzing Power

The analyzing power  $T_{\kappa q}$  of the  $(d, p)$  reaction is given by the expression

$$T_{\kappa q} = \frac{\int d\tau \text{Sp}\{\mathcal{M} \cdot t_{\kappa q} \cdot \mathcal{M}^\dagger\}}{\int d\tau \text{Sp}\{\mathcal{M} \cdot \mathcal{M}^\dagger\}},$$

where  $d\tau$  is the phase volume element,  $\mathcal{M}$  is the reaction amplitude, and the operator  $t_{2q}$  is defined by

$$\langle m | t_{\kappa q} | m' \rangle = (-1)^{1-m} \langle 1 m 1 - m' | \kappa q \rangle,$$

with the Clebsh-Gordan coefficients  $\langle 1 m 1 - m' | \kappa q \rangle$ . The amplitude for the reaction  ${}^1H(d, p)X$  in the light-front dynamics is

$$\mathcal{M}_a = \frac{\mathcal{M}(d \rightarrow p_1 b)}{(1-x)(M_d^2 - M^2(k))} \mathcal{M}(bp \rightarrow p_2 p_3),$$

where  $\mathcal{M}(d \rightarrow p_1 b)$  is the amplitude of the deuteron breakup and  $\mathcal{M}(bp \rightarrow p_2 p_3)$  is the amplitude of the reaction  $bp \rightarrow p_2 p_3$ .

## Light-Front Variables

The ratio

$$\psi(x, p_{1T}) = \frac{\mathcal{M}(d \rightarrow p_1 b)}{M_d^2 - M^2(k)}$$

is nothing but the wave function in the channel  $(b, N)$ ; here  $p_{1T}$  is the component of the momentum  $p_1$  transverse to the  $z$  axis.

The light-front variables  $p_T \equiv p_{1T}$  and  $x$  (the fraction of the deuteron longitudinal momentum taken away by the proton in the infinite momentum frame) are given by

$$x = \frac{E_p + p_{pl}}{E_d + p_d}, \quad k = \sqrt{\frac{m_p^2 + \mathbf{p}_T^2}{4x(1-x)}} - m_p^2,$$

where  $E_d$  and  $p_d$  are the energy and the momentum of the incoming deuteron, respectively,  $p_{pl}$  is the longitudinal component of  $\mathbf{p}_1$ , and  $m_p$  is the mass of the nucleon.

# Relativistic Deuteron Wave Function

The relativistic deuteron wave function in the light-front dynamics was found in ref. [**J. Carbonell and V.A. Karmanov, NP A581(1994)625**]. It is determined by six invariant functions  $f_1, \dots, f_6$ , each of them depending on two scalar variables  $k$  and  $z = \cos(\widehat{\mathbf{k}\mathbf{n}})$ , and has the following form:

$$\psi(\mathbf{k}, \mathbf{n}) = \frac{1}{\sqrt{2}}\sigma f_1 + \frac{1}{2} \left[ \frac{3}{k^2} \mathbf{k}(\mathbf{k} \cdot \sigma) - \sigma \right] f_2 + \frac{1}{2} [3\mathbf{n}(\mathbf{n} \cdot \sigma) - \sigma] f_3 + \frac{1}{2k} [3\mathbf{k}(\mathbf{n} \cdot \sigma) + 3\mathbf{n}(\mathbf{k} \cdot \sigma) - 2\sigma(\mathbf{k} \cdot \mathbf{n})] f_4 + \sqrt{\frac{3}{2}} \frac{i}{k} [\mathbf{k} \times \mathbf{n}] f_5 + \frac{\sqrt{3}}{2k} [[\mathbf{k} \times \mathbf{n}] \times \sigma] f_6.$$

Here  $\mathbf{n}$  is the unit normal to the light front surface, and  $\sigma$  are the Pauli matrices;  $\mathbf{n}$  is defined by

$$(\mathbf{n} \cdot \mathbf{k}) = \left( \frac{1}{2} - x \right) \cdot \sqrt{\frac{m_p^2 + \mathbf{p}_T^2}{x(1-x)}},$$

It will be assumed further that  $\mathbf{n}$  is directed opposite to the beam direction, i.e.  $\mathbf{n} = (0, 0, -1)$ .

# Analyzing Power

The final expression for the analyzing power has the form

$$\begin{aligned}
 T_{2q} \left( \frac{p_{10} d\sigma}{d\mathbf{p}_1} \right)_{un} &= \frac{1}{2(2\pi)^3} \left\{ \frac{I(b, p)}{I(d, p)(1-x)^2} \rho_0(2, q) \sigma(bp \rightarrow p_2 X) \right. \\
 &+ \int \frac{dy d\mathbf{p}_{2T}}{2y(1-y)} \frac{I(b, p)}{(1-y)I(d, p)} \rho_0(2, q) \\
 &\times \left. \frac{p_{20} d\sigma}{d\mathbf{p}_2} (bp \rightarrow p_2 X) [1 + \mathbf{P} \cdot \langle \sigma \rangle] \right\}.
 \end{aligned}$$

$(p_{10} d\sigma / d\mathbf{p}_1)_{un}$	=	cross section for unpolarized deuterons,
$I(b, p), I(d, p)$	=	invariant fluxes of the appropriate particles,
$\langle \sigma \rangle$	=	vector analyzing power of $NN$ -scattering,
$\sigma(bp \rightarrow p_2 X)$	=	total cross section of $NN$ -scattering,
$\mathbf{P}$	=	polarization vector of the nucleon in the deuteron,
$\rho_0(2, q)$	=	density matrices.

## Input Data for Calculations

---

It should be emphasized that the problem has no adjusted parameters. Input data were the following.

- The invariant differential cross sections of processes taking place in the low vertices of the pole diagrams were taken into account according to the known parameterizations [**L.Azhgirey et al.**].

## Input Data for Calculations

---

It should be emphasized that the problem has no adjusted parameters. Input data were the following.

- The invariant differential cross sections of processes taking place in the low vertices of the pole diagrams were taken into account according to the known parameterizations [**L.Azhgirey et al.**].
- To account for the off-shell nature of particle  $b$ , the analytic continuations of the cross section parameterizations to the values of invariant variables  $s' = (b + p)^2$ ,  $t' = (b - p_1)^2$  defined in the low vertex of the pole diagram at  $b^2 \neq m^2$  were used in the calculations.

## Input Data for Calculations

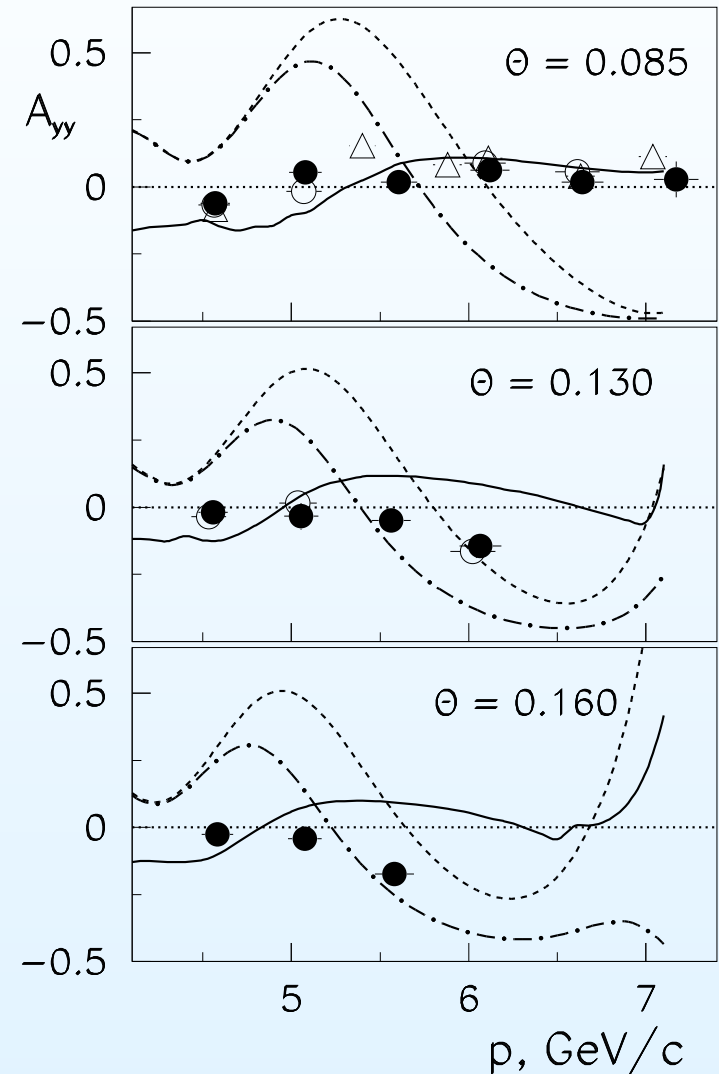
---

It should be emphasized that the problem has no adjusted parameters. Input data were the following.

- The invariant differential cross sections of processes taking place in the low vertices of the pole diagrams were taken into account according to the known parameterizations [**L.Azhgirey et al.**].
- To account for the off-shell nature of particle  $b$ , the analytic continuations of the cross section parameterizations to the values of invariant variables  $s' = (b + p)^2$ ,  $t' = (b - p_1)^2$  defined in the low vertex of the pole diagram at  $b^2 \neq m^2$  were used in the calculations.
- To obtain the values of the invariant functions  $f_i(k, z)$  required for calculations, the spline-interpolation procedure between the table values given in Ref. [**Carbonell and Karmanov, NP A581(1994)625**] was used.

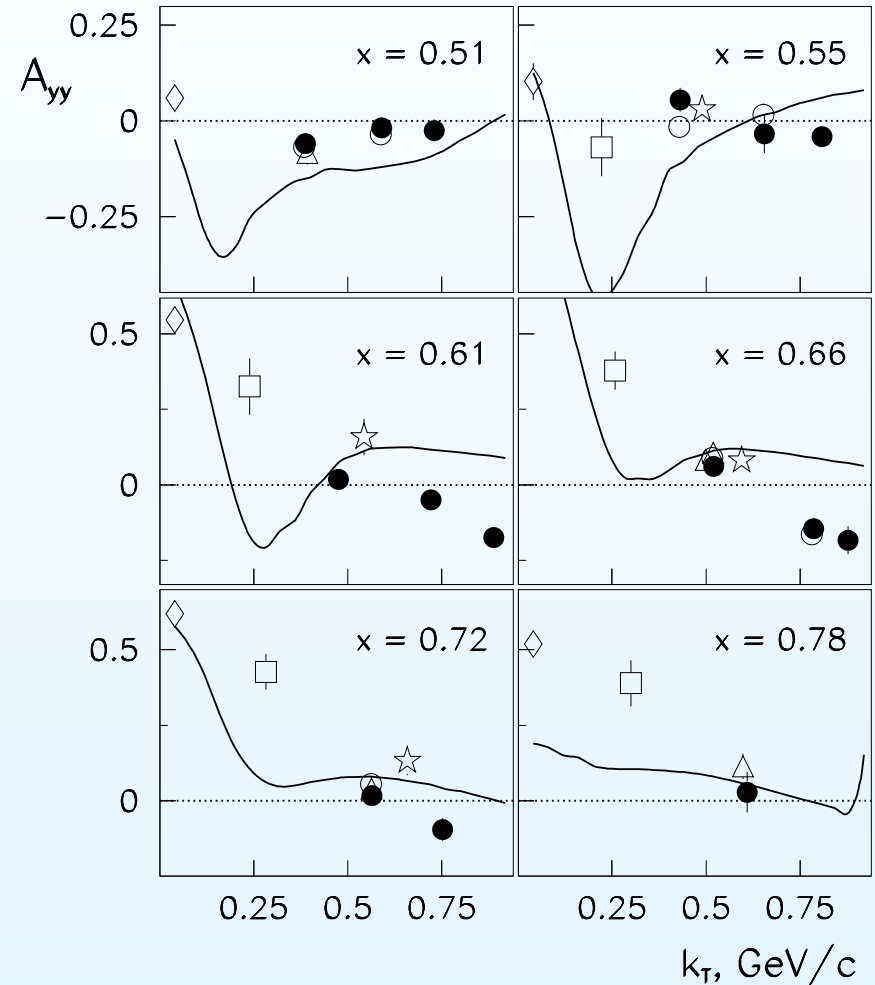
## $A_{yy}$ vs $p$

Data on  $A_{yy}$  of the reaction  $A(d, p)X$  as a function of  $p$  at different angles  $\theta$ . Data were obtained on C at 9 GeV/c at 85 mrad (triangles), on H (light points) and on C (black points) at 85, 130 and 160 mrad. The solid curves were calculated with Karmanov's relativistic deuteron wave function, dashed curves — with DWF for Paris, and point-dashed curves — for Bonn potentials.



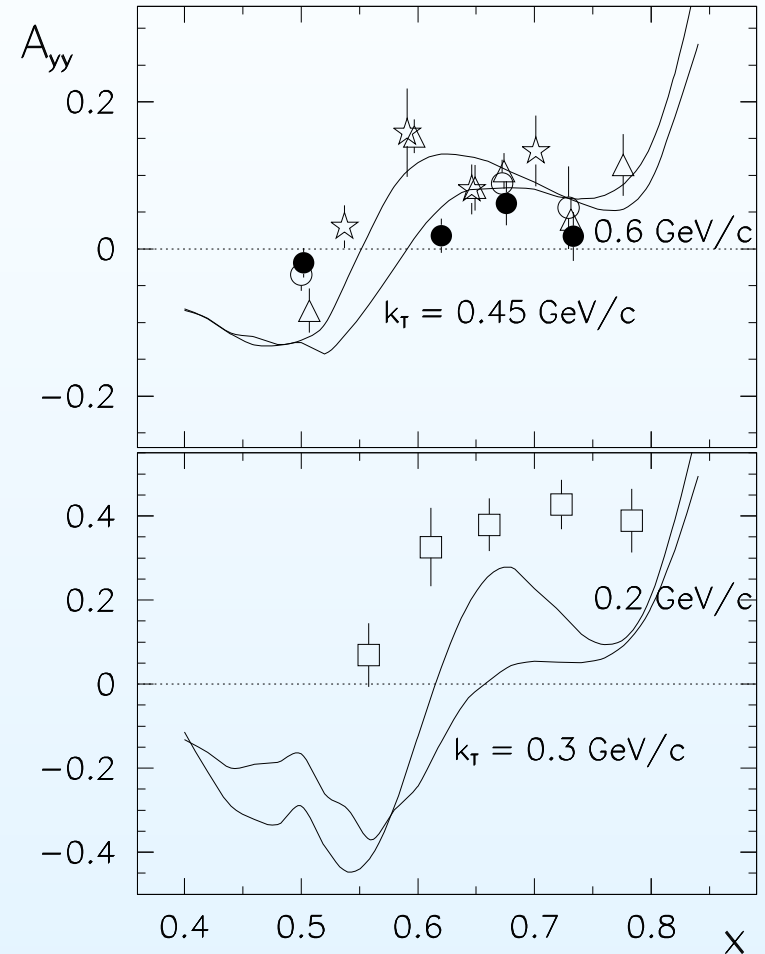
# $A_{yy}$ vs $k_T$

Data on  $A_{yy}$  of the reaction  $A(d, p)X$  as a function of the transverse momentum  $k_T$  near fixed longitudinal momentum fractions  $x \sim 0.51, 0.55, 0.61, 0.66, 0.72$  and  $0.78$ . Data were obtained on C at 9 GeV/c at 85 mrad (triangles), at 85, 130 and 160 mrad (black points), on Be at 4.5 GeV/c and 80 mrad (squares), on Be at 5 GeV/c and 180 mrad (stars), and on C at 9 GeV/c and 0 mrad (diamonds). The solid curves were calculated with Karmanov's relativistic deuteron wave function.



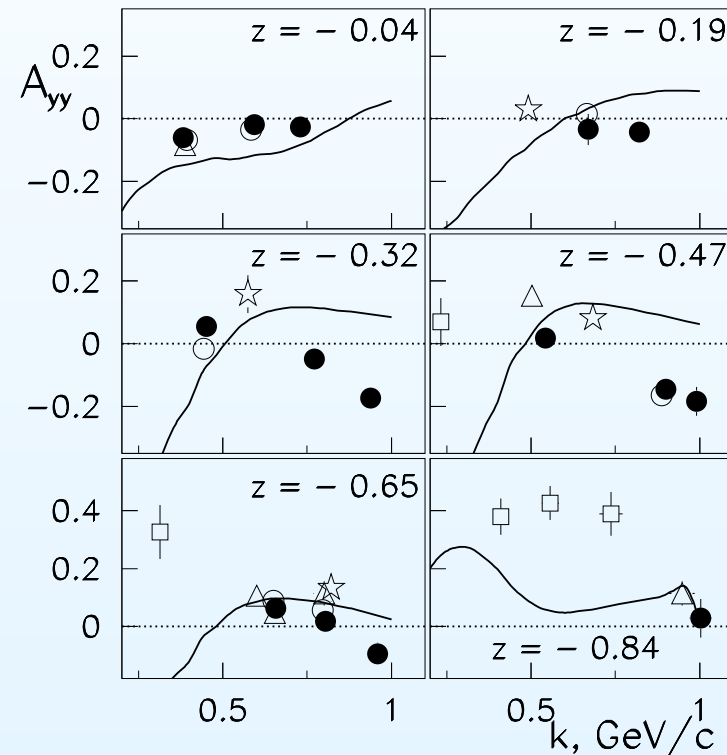
## $A_{yy}$ vs $x$

Data on  $A_{yy}$  of the reaction  $A(d, p)X$  as a function of the longitudinal momentum fractions  $x$  at different transverse momenta  $k_T$ . Data were obtained on C at 9 GeV/c at 85 mrad (triangles), at 85, 130 and 160 mrad (black points), on Be at 4.5 GeV/c and 80 mrad (squares), and on Be at 5 GeV/c and 180 mrad (stars). The solid curves were calculated with Karmanov's relativistic deuteron wave function.



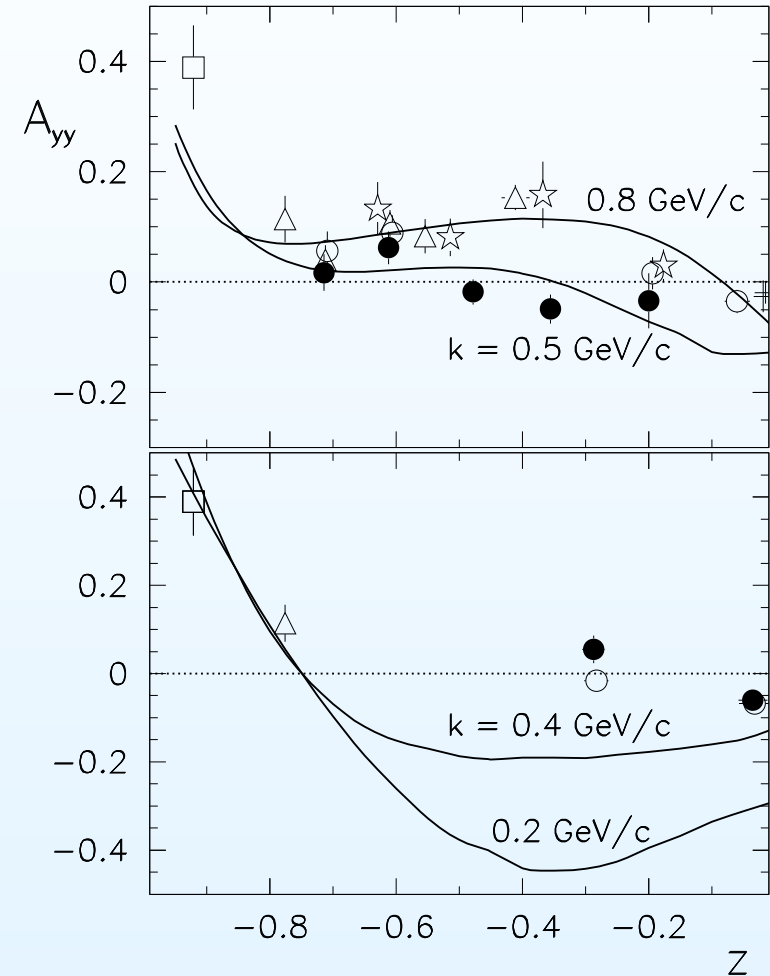
## $A_{yy}$ vs $k$

Data on  $A_{yy}$  of the reaction  $A(d,p)X$  as a function of the momentum  $k$  near fixed values  $z \sim -0.04, -0.19, -0.32, -0.47, -0.68,$  and  $-0.84$ . Data were obtained on C at 9 GeV/c at 85 mrad (triangles), at 85, 130 and 160 mrad (black points), on Be at 4.5 GeV/c and 80 mrad (squares), and on Be at 5 GeV/c and 180 mrad (stars). The solid curves were calculated with Karmanov's relativistic deuteron wave function.



## $A_{yy}$ VS $z$

Data on  $A_{yy}$  of the reaction  $A(d, p)X$  as a function of the value  $z$  at different momenta  $k$ . Data were obtained on C at 9 GeV/c at 85 mrad (triangles), at 85, 130 and 160 mrad (black points), on Be at 4.5 GeV/c and 80 mrad (squares), and on Be at 5 GeV/c and 180 mrad (stars). The solid curves were calculated with Karmanov's relativistic deuteron wave function.



## Conclusion

---

- A wide range of problems associated with the investigation of the structure and dynamics of relativistic deuterons in  $(d, p)$  processes on nucleons and nuclei has been considered.

## Conclusion

---

- A wide range of problems associated with the investigation of the structure and dynamics of relativistic deuterons in  $(d, p)$  processes on nucleons and nuclei has been considered.
- Experimental data include the momentum distributions of protons, along with the tensor analyzing power of these reactions on different nuclei and at different energies, measured on the beams of unpolarized and polarized deuterons at the JINR Synchrophasotron.

## Conclusion

---

- A wide range of problems associated with the investigation of the structure and dynamics of relativistic deuterons in  $(d, p)$  processes on nucleons and nuclei has been considered.
- Experimental data include the momentum distributions of protons, along with the tensor analyzing power of these reactions on different nuclei and at different energies, measured on the beams of unpolarized and polarized deuterons at the JINR Synchrophasotron.
- When interpreting experimental results, the accent is made on making use of the LF dynamics because the employment of this dynamics allows the data to be analysed in terms of a wave function.

## Conclusion

---

- A wide range of problems associated with the investigation of the structure and dynamics of relativistic deuterons in  $(d, p)$  processes on nucleons and nuclei has been considered.
- Experimental data include the momentum distributions of protons, along with the tensor analyzing power of these reactions on different nuclei and at different energies, measured on the beams of unpolarized and polarized deuterons at the JINR Synchrophasotron.
- When interpreting experimental results, the accent is made on making use of the LF dynamics because the employment of this dynamics allows the data to be analysed in terms of a wave function.
- It is shown that with this approach new important information on the deuteron structure at short distances can be obtained, and the deuteron behaviour at relativistic energies may be adequately described.

## Account of Relativity

---

- A general approach to the description of relativistic quantum phenomena has to be based on the representations of the Poincaré group.
- Fundamental degrees of freedom — quarks, leptons, and gluons — should be described by the wave functions, which are the irreducible representations of the Poincaré group, in conformity with the generally accepted ideas.
- Here we deal with effective degrees of freedom — hadrons. We also consider hadrons as the irreducible representations of the Poincaré group. The basic analysis is carried out within the framework of the light-front dynamics.

## Momentum Spectra

---

- Data on the momentum distributions of protons emitted in the  $A(d, p)X$  reactions are well described within the framework of the LF dynamics even with the use of non-relativistic DWF transformed in an appropriate way when passing in the moving-deuteron system.
- In this case, the agreement with the experimental data takes place up to proton transverse momenta of 0.5–1 GeV/ $c$ .
- This means that the nucleons retain their individuality in the region where they should overlap, and it is seemingly difficult to justify the use of the concept of the wave function.

## Analyzing Powers

---

- In the case of the tensor analyzing power  $A_{yy}$  of the  $A(d, p)X$  reaction, it is possible to speak only about the qualitative agreement between the experimental data and their description using Karmanov's relativistic DWF.
- In this connection, we note that taking into account the simple pole diagram is of a trial nature in our approach; however, the calculations are consistently relativistic, and, in the future it would be possible to add supplementary contributions for better understanding what happens to the deuteron in the case of the relativistic internal and external momenta.